2018 Problem 7: Conical Piles

Heron's Fountain

Alvin Ling

Department of Physics, University of Chicago, Chicago, IL 60637, U.S.A.

E-mail: linga@uchicago.edu

Yu-Wei William Hsieh

Department of Physics, National Taiwan University, Taipei 10617, Taiwan (ROC)

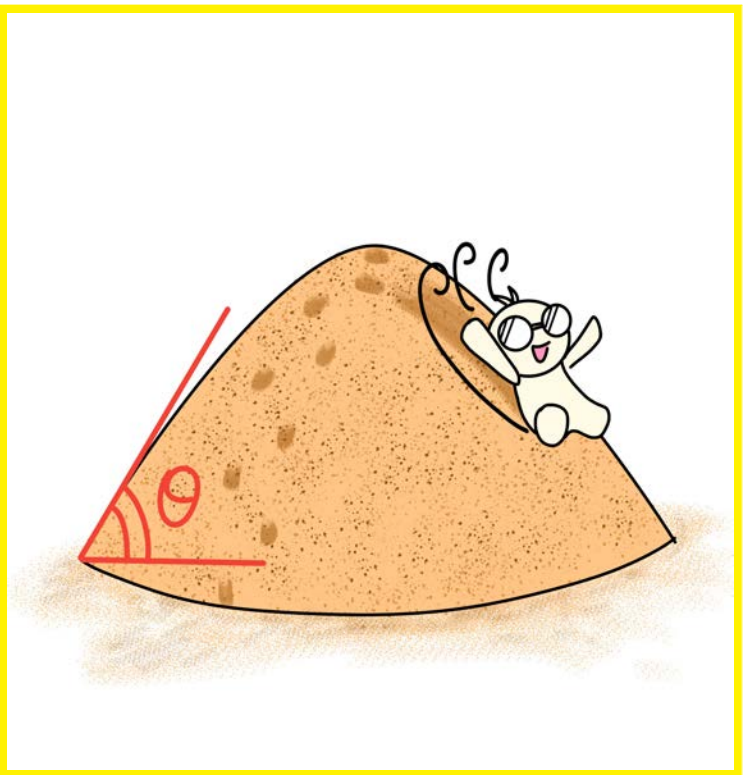

Abstract

This paper conducts a detailed investigation into the formation of conical piles from non-adhesive granular materials, tracing the process from the development of the initial plate to the tapering of the pile's end region. Phenomenological observations of the former are understood through the energy content of the granular particles; the relation of the annular wall's outer radius to the nozzle height given by this approach is empirically confirmed. Next, the Bak-Tang-Wiesenfield (BTW) Abelian Sandpile Growth model is evaluated and refined through considerations for elasticity rising from the packing patterns of granular particles. The derived, time-independent recursive model for the growth of the main pile is subsequently verified through cross-referenced values for Young's Modulus. Additional corrections are made for the dipping pattern caused by stress from the falling particles to resolve experimental discrepancies. Finally, the aforementioned tapering at the end regions are theoretically modelled with a stochastic probability distribution based on the continued fall of sand particles.

1 Nomenclature and Preliminary Experimental Setup

Prior to the actual investigation on the conical pile, there are several terms that should be defined. The rest angle is defined as the angle of the slope of the sand pile, as

$$\theta_{rest} = \arctan\left(\frac{dy}{dx}\right) \tag{1}$$

Qualitatively, the rest angle is the slope of the static sandpile, hence the angle at which the sand particle will remain stationary. On the contrary, the angle of repose is defined as the maximum angle such that the sand particle will remain in the pile. While the rest angle may be different for all sandpiles, the angle of repose will be constant given certain parameters of discussion in Section 4.

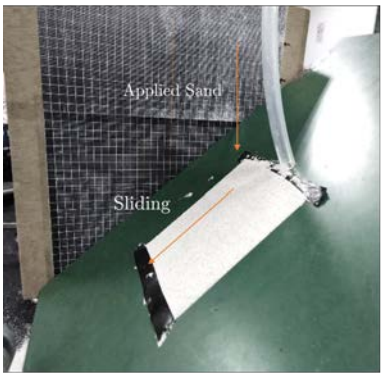

FIG. 1. Experimental Apparatus to test the angle of repose of a granular system.

Therefore, based on the principle of static equilibria, $N = mg\sin\theta$ and $\mu N = mg\cos\theta$. Therefore, $\mu \approx \tan\theta$. Since the sand particle would not be moving if it is on the angle of repose, $\theta = \tilde{\theta}$ and $\mu = \mu_s$.

$$\tilde{\theta} \approx \arctan\mu_s \tag{2}$$

It is possible to experimentally test the angle of repose of a sand pile through the apparatus demonstrated in Figure 1. The apparatus contains sand particles fixed by double sided adhesive tape to simulate the maximum static coefficient, μ_s of sand. As extra sand is applied on the board, if the board is angled greater than the angle of repose, then by the definition of the angle of repose, the sand particles would naturally slide downwards. The pipe contains a release mechanism that releases sand by a slit to ensure consistency in the experiment.

The angle of repose of the controlled sand is measured to be 35.11° from the ground. The experimental apparatus based on Figure 2 is used to accurately measure the shape of a sandpile and its time evolution is shown in Figure 2. The typical sand used in the investigation is quartz sand retrieved from a beach with an approximate Young's modulus of 55 MPa and granular size of 1.5 mm. From the apparatus, it is possible to measure the

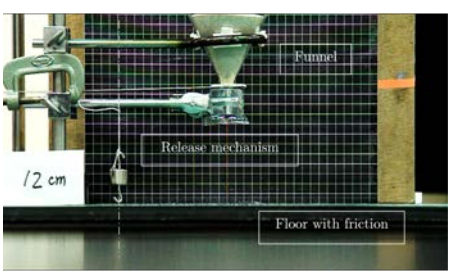

FIG. 2. Experimental apparatus of measuring the shape of the conical pile.

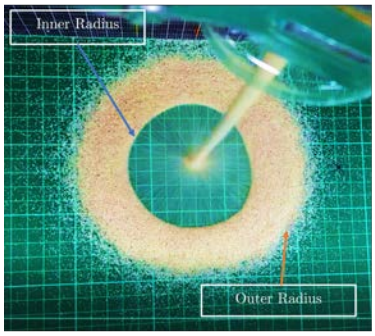

FIG. 3. The formation of the bottom of the conical pile.

shape of a sand pile. In the preliminary stage of the investigation, three experiments with sandpiles of controlled amount of the control sand released from the same height were performed. While the three experiments does suggest similar dynamics, there are often minor variations on the top of the sandpile, demonstrating that sandpile formation is itself a stochastic process.

2 The Formation of the Initial Plate of a Sandpile

As sand particles are falling from the apparatus, sand bounced away from center created an annular wall and evolved into a plateau, as seen in Figure 3. Consider the graph of the inner radius, as defined in Figure 3, versus time. The incline in the inner radius of the conical pile implies that each individual sand particle is flying, sliding, and rolling. The peak of Figure 4 is observed as an aannular wall appears in the front, as the outer radius of the pile is fixed. The negative slope after the peak in Figure 4 demonstrate the conservation of momentum as sand particles collides and bounces back from the annular wall formed. The formation of the annular wall is again empirically verified in Figure

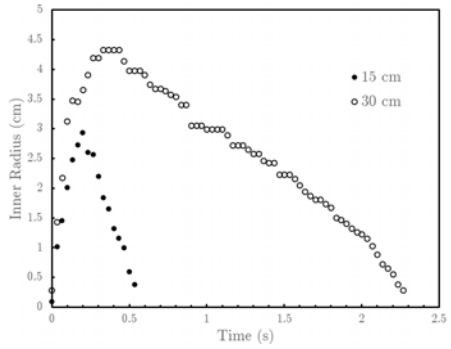

FIG. 4. Inner radius of the conical pile during formation versus time for two different initial heights.

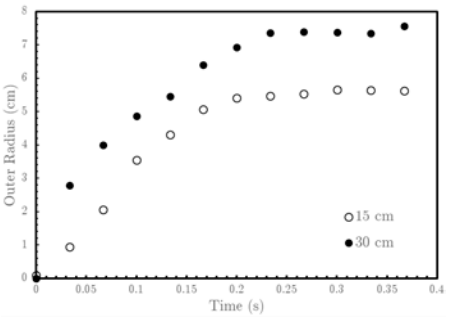

FIG. 5. Outer radius of the conical pile during formation versus time for two different initial heights.

5.

As previously mentioned, the mechanism of initial pile formation is due to the conversion of potential and kinetic energy as sand particles drop from the nozzle. As the potential energy, due to the height of the funnel, increases, the nozzle outer radius increases. Therefore, the outer radius term would be proportional to the sum of various energy terms,

$$R_{out} = \alpha(2h\sin 2\theta) + \sqrt{\frac{\alpha^2 mgh}{\mu}} + C \qquad (3)$$

Note that the theory curve does not cross the y-axis: the valid region only range from the intersection between the R_{out} curve and the line $R_{out} = H$, up until the point where the sand particles will reach terminal velocity. Note that α corresponds to the coefficient of restitution of sand particles to the ground, and μ is the coefficient of kinetic friction, and θ corresponds to the average restitution angle, which would, in most case, be near 0°. Note that while the coefficients mentioned above are experimentally difficult to yield, the theoretical graph matches very well with the experimental graph proposed in Figure 6.

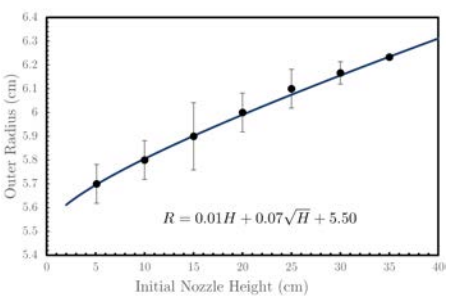

FIG. 6. The outer radius of the conical pile during formation versus the height of the nozzle.

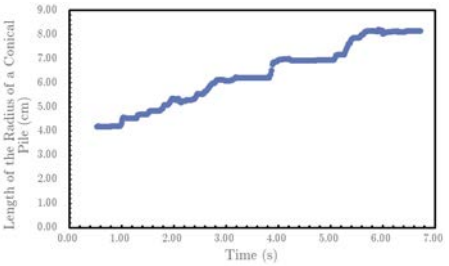

FIG. 7. The Growth of a 200 g conical pile, dropped from 10 centimeters above.

3 The Growth of the Sandpile after the formation of the Initial Plate

The formation of the mother pile should be in accordance to the theory predicted by the Bak-Tang-Wiesenfield Abelian Sandpile Growth model (BTW) [1]. The Abelian sandpile model predicted that even when the conditions are exactly satisfied without scaling for probability, the angle of repose does not equal to the rest angle, or the angle the conical pile makes with the ground away from the end section. The model follows three simple rules:

$$\begin{cases} z_0 - z_1 > C_N \\ z_0 = z_0 - 1 \\ z_1 = z_1 + 1 \end{cases} \qquad (4)$$

This model works as it simulates the definition of the angle of repose – it is the maximum angle in which sand will remain still on a conical pile. The critical value of this model corresponds to the angle of repose – in which the stillness gets disrupted, causing the sand particle on the top layer collapse into the bottom layer, which then continues to collapse until no angle goes higher than the angle of repose. The avalanche is caused by the instability of the pile after the stacking of the sand particles

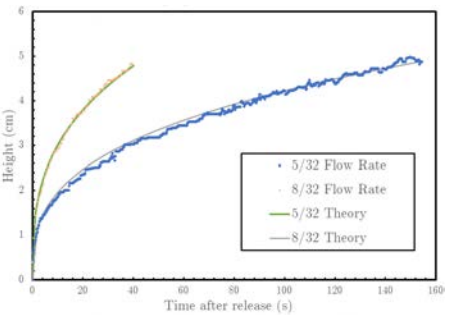

FIG. 8. Height of the conical pile for different nozzle radius (cm) versus time (sec) after release.

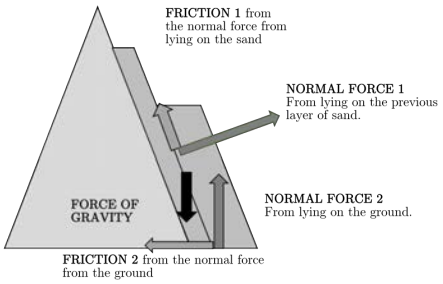

FIG. 9. Free body diagram on two discrete layers on a sand pile.

exceed the critical value (or the angle of repose).

There is empirical implication that serves as evidence for the validity of the BTW model from Figure 7. The radius of a conical pile grows near linearly until it reaches outer radius. Moreover, as more sand particles accumulate such that $\tan\theta > \mu_s$ sand particles rolls off the pile to the floor, adding radius, simulating the modification of z_0 and z_1 in the BTW model. It is possible to empirically predict the height of a conical pile. Note the contrast between Figure 7 and 8, that while avalanches are widely seen in Figure 7 (horizontal), but the height is not significantly affected by the avalanches, as seen in Figure 8. This is again, due to having only the outermost layer of the conical pile involved in actual avalanches, while the inner layers generally are more stable. The height of the Conical Pile can be predicted as

$$\begin{aligned} V &= \frac{1}{3}\pi r^2 h \\ &\implies h = \frac{1}{C_N}\sqrt[3]{\frac{3Qt}{\pi C_N}} = \frac{1}{C_N}\sqrt[3]{\frac{3V}{\pi C_N}} \end{aligned} \tag{5}$$

In the equation above, C_N is the critical number stemming from the angle of repose, which is equivalent to the critical number employed in the BTW model:

$$C_N = \tan\tilde{\theta} \tag{6}$$

However, there remain a crucial erroneous assumption made by the BTW model - the BTW Model assumes that all sand particles are equally spaced in a sand pile. However, in reality, the sand particles will organise themselves into more densely packed piling pattern when an exterior force is applied on the pile, similar to the mechanics of elastic objects [2]. Note that it is at this point where the research will transform from phenomenological observations into quantitative analysis.

4 Investigation on the shape of a Sandpile through the Elastic Modulus

Consider the forces interacting between two kinks and the floor. Let θ be the angle of repose, which is the angle of the normal force for all piles. There are internal forces in the pile [2]. The forces present are demonstrated in Figure 9. The condition for static equilibrium occurs when there's no net force, thus, solving for the normal force on a kink yields

$$\begin{cases} N_1 = \frac{mg\mu_2}{(\mu_2-\mu_1)\cos\theta+(\mu_1\mu_2+1)\sin\theta} \\ N_2 = \frac{mg(\mu_2\cos\tilde{\theta}-\mu_2\cos\tilde{\theta}+\sin\tilde{\theta})}{(\mu_2-\mu_1)\cos\theta+(\mu_1\mu_2+1)\sin\theta} \end{cases} \tag{7}$$

The mass of the kink can be represented by the product of density and volume. Thus, using a Jacobian matrix,

$$\begin{aligned} \Delta m &= \rho\Delta V = \rho\Delta x\Delta y\Delta z = \rho r\Delta r\Delta\theta\Delta z \\ &= \frac{1}{2}\rho(l_f - l_i)(l_i)(2\pi)(h_i) \end{aligned} \tag{8}$$

Where the 1/2 comes from the fact that the kink takes the shape like that of a triangle. Thus, the system converts into [3]

$$\begin{cases} N_1 = \frac{2\pi\rho g\mu_2}{(\mu_2-\mu_1)\cos\theta+(\mu_1\mu_2+1)\sin\theta}(l_f - l_i)(l_i h_i) \\ N_2 = \frac{2\pi\rho g(\mu_2\cos\tilde{\theta}-\mu_1\cos\tilde{\theta}+\sin\tilde{\theta})}{(\mu_2-\mu_1)\cos\theta+(\mu_1\mu_2+1)\sin\theta}(l_f - l_i)(l_i h_i) \end{cases} \tag{9}$$

The surface area is the volume without the "thickness". Thus,

$$Adl = \frac{\partial V}{\partial l_i} = (l_f - l_i)(2\pi)(h_i)dl_i \tag{10}$$

$$Adh = \frac{\partial V}{\partial h_i} = \left(\sum_{n=0}^{i} l_n\right)(2\pi)(d_i)dh_i \tag{11}$$

Note that the differential total surface area is

$$dV = \frac{\partial V}{\partial l}dl + \frac{\partial V}{\partial\theta}d\theta + \frac{\partial V}{\partial z}dz \tag{12}$$

Thus, when there's no change in one variable, the other variables can be completely neglected. From the free-body diagram, realize that the friction generated by the normal force of the $(i+1)$th kink is compressing the ith kink. Thus, by the relationship of stress and strain, in which the product of modulus and stress equals to strain,

$$E\int_{l_{i+1}}^{l_i}\frac{dl_n}{l_n} = -\mu N_2\frac{1}{A} \tag{13}$$

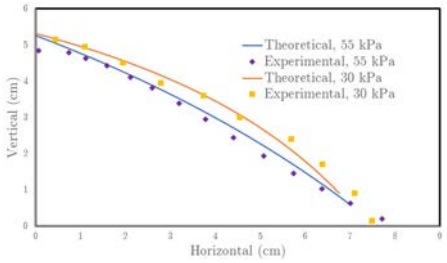

FIG. 10. Two different sandpile with different Young's Modulus.

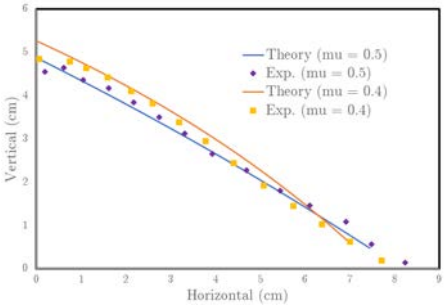

FIG. 11. Two different sandpile with different ground friction.

Thus, yields a relationship

$$E \ln \frac{l_{i+1}}{l_i} = -\frac{\pi \rho g \mu_2}{(\mu_2 - \mu_1)\cos\theta + (\mu_1\mu_2 + 1)\sin\theta} l_i \tag{14}$$

Similarly, from the free-body diagram, realize that the frictional force of the $(i+1)$th kink is stretching the ith kink. Thus, by the relationship of stress and strain,

$$\begin{aligned} E\int_{h_n}^{h_{n+1}} \frac{dh_n}{h_n} &= \mu N_1 \frac{1}{A} E \ln \frac{h_{n+1}}{h_n} \\ &= \frac{\mu_2 \cos\tilde{\theta} - \mu_1 \cos\tilde{\theta} + \sin\tilde{\theta}}{(\mu_2 - \mu_1)\cos\theta + (\mu_1\mu_2 + 1)\sin\theta} (h_{n+1}) \end{aligned} \tag{15}$$

In summary, the system of solution yields

$$\begin{cases} l_{i+1} = l_i \exp\left(-\frac{\rho g \mu_2 \sin\tilde{\theta}}{E[(\mu_2-\mu_1)\cos\tilde{\theta} + (\mu_1\mu_2+1)\sin\tilde{\theta}]} l_i\right) \\ h_i = h_{i+1} \exp\left(-\frac{\rho g(\mu_2\cos\tilde{\theta} - \mu_1\cos\tilde{\theta} + \sin\tilde{\theta})}{E[(\mu_2-\mu_1)\cos\tilde{\theta} + (\mu_1\mu_2+1)\sin\tilde{\theta}]} h_{i+1}\right) \end{cases} \tag{16}$$

Let $l(i)$ and $h(i)$ be functions of the given recursion. The sand pile will have a curve following the shape of $(x,y) = (l_f - l(i), h(i))$. Thus, the area of the sand pile would be

$$A = \sum_i h_i (i_i - l_{i+1}) \tag{17}$$

In terms of general assumptions, the computer generation of x should be negated, as in following the previous redefinition of x in terms of l. Moreover, the generation of y should be inverted, since the h is almost a reverse recursive relation. We can simply let our initial term, h_0, be the term that we are seeking for, and let the first term that we evaluate be the smallest height that is possible to exist in a sand pile, being one particle of sand itself. I now hypothesize that the formation of y would be an invariant – the initial height would always be the same, and solely depends on when the minimum is reached by the x.

Equation 16, being of the shape of a conical pile, can easily be verified experimentally. As the equation proposed is not time dependent, the experimental result is only measured when all of the sand particles drop onto the conical pile.

The experiment demonstrated by Figure 10 and 11 is analyzing the curve formed by different materials and floor friction. Due to the poor technique of experimental performance, the precision of the received Young's Modulus (E) is approximately 2 kPa, with cross referencing from outside sources [4]. The Young's Modulus yielded in this experiment is both experimentally yielded and verified through literature. Experimentally, the Young's Modulus is yielded by placing a collection of sand particles in a large cylinder, then placing a large mass on top of the cylinder. The elastic modulus is yielded by the ratio of the measured strain versus the measured strain.

The solid line on Figure 10 and 11 represent the theoretical prediction, with the fitted equation marked in the figure. The experimental points are represented as points on the graph. Since the theoretical and experimental values clearly match, it can be concluded that the theoretical derivation proves accurate. It is observed that when the Young's Modulus (from packing) is higher, the curvature of the sand pile is higher. This occurs because when the modulus is higher, the sand layers themselves are packed more stiff, thus is harder to deform. Moreover, the radius of the sand pile with lower friction is higher, as it requires more energy for individual sand particle to overcome higher friction of the floor, thus less kinetic energy is available for individual sand particles to overcome the lost energy due to friction.

However, there exists a discrepancy between the theoretical and experimental data during the initial region (when horizontal direction is small) due to the effects of dipping, in which the change of momentum from the falling sand adds an extra force on the top of the pile. As the theory predicts that the sand pile is a solid with an elastic modulus, it is possible to establish an equation creating the link between the displaced height versus the stress due

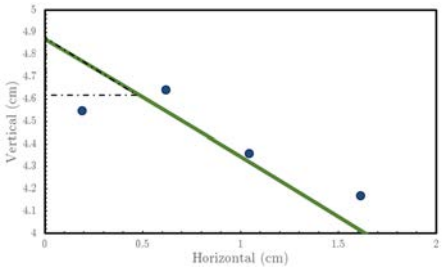

FIG. 12. Rough sand dropped from 52 cm at 0.45 coeff. of friction, Repeated.

to the falling $n = \frac{r^2}{r_{sand}^2}$ sand particles.

$$\Delta h = \frac{h_0}{AE}\left(\frac{r_{nozzle}^2}{r_{sand}^2}\right)\frac{m_{sand}gt}{\Delta t} \tag{18}$$

The volume of the pile should not change if a pressure dip is created. Therefore, using the above recursion, it is possible to rewrite the conservation of volume into the Equation 19.

$$2\sum_i h_i(l_i - l_{i+1}) = 2\left[h_0\Delta l + \sum_{i+1}(l_i - l_{i+1})h_i\right] - 2\frac{\Delta h\Delta l}{2} \tag{19}$$

Thus proposing a net equation considering the effects of avalanching.

$$\begin{cases}\Delta h = \frac{h_0}{AE}\left(\frac{r_{nozzle}^2}{r_{sand}^2}\right)\frac{m_{sand}gt}{\Delta t} \\ \Delta l = \frac{2h_0(l_0 - l_k)}{2h_0 - \Delta h}\end{cases} \tag{20}$$

By repeating Figure 9 again, but zoomed onto the initial region (Figure 12), one can make an approximation on the size pressure dipping. The triangle created by the dashed line represents the area affected by the pressure dip, and the horizontal leg of the pressure dip triangle is the approximated new height of vertical length of the sand pile within the region of the sand pile.

5 Correction of the sandpile model in the end section

Define ending part of the conical pile as the area where $\theta < \tilde{\theta}/2$. Since the gravitational potential at the end section would be relatively similar, since they are relatively distributed on similar height – the probability that one sand particle would fall from one layer to another would be p, hence the probability that a particle would stay on a layer would be $1 - p$, as represented with a schematic diagram in Figure 13. [5]

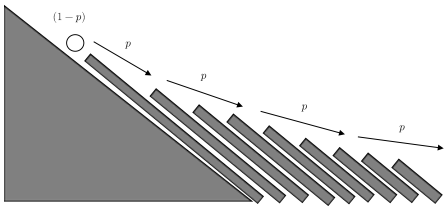

FIG. 13. Stochastic Model on the End Pile Correction.

From the analysis above, the height of the pile at x should follow the equation

$$y = \frac{B}{A}(1-p)(p^x) \tag{21}$$

Where B is proportional to the size of end portion, and A is the normalization constant. From Figure 14, which itself is a zoom into the experiment from Figure 9 at the end region, demonstrates a correlation between the end pile and the probabilistic model, albeit that further adjustments may be required.

6 Conclusion

In terms on the formation of sand pile, the inner radius expand with outer radius (incline), while declines by filling the annular wall formed by the boundary of the outer radius. The outer radius can be approximated as

$$R_{out} = \alpha(2h\sin 2\theta) + \sqrt{\frac{\alpha^2 mgh}{\mu}} + C \tag{22}$$

In which the α and C constants may be fitted for different empirical settings.

The formation of the conical pile is also in accordance to the BTW Abelian Sandpile Model, in

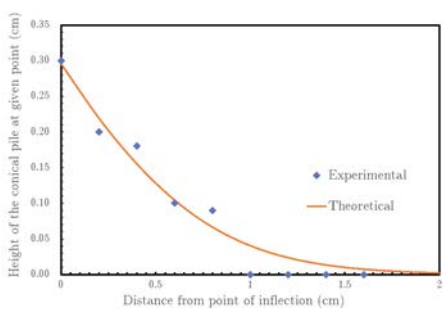

FIG. 14. Experiment from Figure 9 zoomed to investigate the fitting of ending part of the conical pile based on probablistic model.

which there will then be growths of the inner radius due to avalanches. Due to the effects of packing and static equilibria, the sandpile will demonstrate different shapes in the initial dipping, middle, and the end pile regions. The middle region carries the shape described by the recursion

$$\begin{cases} l_{i+1} = l_i \exp\left(-\frac{\rho g \mu_2 \sin\tilde{\theta}}{E[(\mu_2-\mu_1)\cos\tilde{\theta}+(\mu_1\mu_2+1)\sin\tilde{\theta}]} l_i\right) \\ h_i = h_{i+1} \exp\left(-\frac{\rho g(\mu_2\cos\tilde{\theta}-\mu_1\cos\tilde{\theta}+\sin\tilde{\theta})}{E[(\mu_2-\mu_1)\cos\tilde{\theta}+(\mu_1\mu_2+1)\sin\tilde{\theta}]} h_{i+1}\right) \end{cases} \tag{23}$$

The initial dipping region, as caused by the forces of the falling sand, will carry the shape of the triangle

$$\begin{cases} \Delta h = \frac{h_0}{AE}\left(\frac{r_{nozzle}^2}{r_{sand}^2}\right)\frac{m_{sand}gt}{\Delta t} \\ \Delta l = \frac{2h_0(l_0-l_k)}{2h_0-\Delta h} \end{cases} \tag{24}$$

And the end pile region demonstrates that of a stochastic probability distribution,

$$y = \frac{B}{A}(1-p)(p^x) \tag{25}$$

References

[1] Bak P., Tang C. & Wiesenfeld K. (1987). Self-organized criticality: An explanation of the 1/f noise. Phys. Rev. Lett. 59(4), 381–384. Doi:10.1103/physrevlett.59.381

[2] Herrmann H. J.(1998). On the Shape of a Sandpile. Physics of Dry Granular Media, 319-38.

[3] Taylor, John R. (2005). Classical Mechanics. Sausalito, CA: Univ. Science Books.

[4] 2010. Some Useful Numbers on the Engineering Properties of Materials. Data Sheet, Austin, TX: Jackson School of Geology, University of Texas at Austin.

[5] Alonso J. J. and Herrmann H. J. (1996). Shape of the tail of a two-dimensional sandpile. Phys. Rev. Lett. 76(26), 4911.

[6] Courteous guidance from Mr. Adrian Nolin (Taipei American School), Dr. Allan Bayntun (Taipei American School), Dr. Fang-Yu Luh (National Taiwan Normal University), Dr. Vincent Yeh (Donghua University, Hualien) and Dr. Yung-Yuan Hsu (National Taiwan Normal University).